

## PAPER

# Advancements in Breast Cancer Detection through Broadband Microstrip Antenna Technology

Amer Alsaraira<sup>1</sup>(✉), Omar  
A. Saraereh<sup>2</sup>, Samer Alabed<sup>1</sup>

<sup>1</sup>Biomedical Engineering  
Department, School of  
Applied Medical Sciences,  
German Jordanian University,  
Amman, Jordan

<sup>2</sup>Department of Electrical  
Engineering, Faculty of  
Engineering, The Hashemite  
University, Zarqa, Jordan

[amer.alsaraira@gnu.edu.jo](mailto:amer.alsaraira@gnu.edu.jo)

## ABSTRACT

In this paper, a novel method for detecting breast cancer utilizing an ultra-wideband (UWB) microstrip patch antenna operating in the UWB frequency range is presented. The promise of non-invasive, radiation-free breast cancer screening is provided by UWB technology. We give a brief overview of the difficulties in detecting breast cancer as well as the benefits of UWB technology in medical applications in this study. This study presents a compact printed microstrip patch antenna used for the bio-medical application at industrial, scientific, and medical (ISM) and UWB frequencies. The proposed antenna consists of a hexagonal-shaped microstrip patch antenna with a slotted ground antenna used for high bandwidth for a wider range of applications. The compact biomedical antenna is printed on Roger 5880 substrate with an overall dimension of 25\*25 mm. Due to the high demand for results accuracy, Roger 5880 substrate material is used because it has good dielectric characteristics and loss factors that are appropriate for medical and radio frequency (RF) applications. A 50-ohm impedance line is used to feed the antenna. The proposed antenna has a higher bandwidth of almost 12.5 GHz at such a low frequency, starting from 3.53 to 16 GHz. The antenna has an acceptable gain of 3.38 Db, which is enough for the required application. The UWB microstrip patch antenna has the potential to improve breast cancer detection accuracy and reliability, which would aid in early diagnosis and better cancer patient treatment. This work represents a major advancement in the development of non-invasive, low-cost breast imaging methods for early cancer diagnosis.

## KEYWORDS

ultra-wideband (UWB) antenna, cancer patient, sustainable fabrication, bio-medical application, good health and well-being

## 1 INTRODUCTION

In the realm of biomedical engineering, antenna design is essential, especially for applications such as breast tumor detection where accurate and non-invasive procedures are required. The designed antenna, which was made possible by the

Alsaraira, A., Saraereh, O.A., Alabed, S. (2024). Advancements in Breast Cancer Detection through Broadband Microstrip Antenna Technology. *International Journal of Online and Biomedical Engineering (iJOE)*, 20(13), pp. 41–59. <https://doi.org/10.3991/ijoe.v20i13.50509>

Article submitted 2024-06-10. Revision uploaded 2024-08-14. Final acceptance 2024-08-14.

© 2024 by the authors of this article. Published under CC-BY.

CST Studio Suite, is an illustration of a methodical and thorough approach that concentrates on providing broadband capabilities that are essential for achieving the kind of penetration depth and resolution that are critical in medical imaging applications. Rogers RT5880, which combines downsizing with bandwidth optimization and has a favorable dielectric and loss factor, makes up the antenna's substrate. The patch's copper fabrication and hexagonal shape ensure low signal loss and effective transmission, and its exact geometric features- such as its 12 mm radius are thoughtfully engineered to best influence the resonance frequency and radiating characteristics. The feed line ensures a straight and efficient connection to the hexagonal patch; it must meet certain requirements for thickness and length. The ground plane is made of copper-annealed, and its specific dimensions and slots (which are square and rectangular) influence the radiation pattern and impedance of the antenna in addition to increasing its radiation efficacy.

The significance of antennas in the imaging process cannot be overstated, as they are required to function near the body due to link budget constraints. [1]. The first technique often uses only the far-field characteristics because there are few widely accepted near-field figures of merit to guide the antenna selection and design for sustainable manufacturing. Phase linearity across the bandwidth [2], unidirectional beam [3], and radiation pattern stability are the criterion points. Additional requirements include very wide impedance bandwidth, high pulse fidelity [4], and low pulse stretch, which are influenced by near-field obstacles but do not necessarily depend on the observation distance.

Antennas used for mm wave often aim to achieve the best possible balance between the specifications. Bowties [5, 6], planar dipole [7], monopole [8, 9], slot-based [10], inverted-F [11, 12], and the horn [13] antennas are a few examples. Active circuit-backed electrically short antennas are another way to improve antenna miniaturization [14]. Patch antennas are extremely popular these days since they are simple to make and can be adjusted without replacing the entire antenna. Its inexpensive price, lightweight, and low profile are other benefits. Nevertheless, it has certain shortcomings, such as a small bandwidth and poor gain. A multitude of techniques are developed for patch antennas to enhance their bandwidth and gain. The EBG structure is one technique [15]. The most ideal antenna is the microstrip antenna because of its appropriate unidirectional radiation pattern, which reduces the user's exposure to electromagnetic radiation [16].

The development of antennas for the industrial, scientific, and medical (ISM) band at 2.45 GHz is the foundation of this study [17]. The creation of new electromagnetic band gap antenna types can be considered a significant endeavor to increase the antenna's gain and bandwidth [18]. Tablets and laptops that are nearby are ideal for connecting across the 5.8 GHz frequency spectrum. It is a better option for high-frequency trading and other data-intensive operations since it is less crowded than other frequency bands [19].

Microstrip filter-antenna designs have gained popularity recently as some of the most sought-after radio frequency (RF) structures due to their small size, lightweight nature, low profile, and ease of fabrication [20, 21, 22]. It is well known that using a substrate material presents a number of significant difficulties when designing RF and microwave circuits. Selecting the right substrate material type and thickness for a given application is one of the fundamentals of design [23]. Antennas that can operate at two different frequencies simultaneously are known as dual band microstrip patch antennas. Their adaptability is useful in situations requiring the use of several frequencies, such as radar systems, wireless networks, and satellite communications [24].

However, there is a broad spectrum of frequencies and bandwidths covered by IoE applications; therefore, antennas must be specifically constructed for these needs at those frequencies and bandwidths. Recently, there has been a lot of interest in a frequency range centered at 5.8 GHz that is based on the license-free ISM band. Many research organizations have worked toward increasing microstrip antenna response to this frequency because it is now relatively unfettered and allows for broader bandwidths [25, 26, 27, 28].

Lightweight, small antennas that are cheap, environmentally friendly, have good gain values, high efficiency, and may sometimes operate in many bands or on a wideband are necessary for wireless communications. Printed circuit board (PCB) antennas can lower design costs and meet all requirements. PCB antennas do, however, have the drawback of significantly increasing pollution because of the lithographic process that is required. Furthermore, the characteristics of most commercial substrates limit the flexibility of design [29, 30, 31]. However, 3D printing technology is a prototyping approach that has gained prominence in recent years because it can easily and quickly create complex 3D structures at a cheap cost while also being ecologically benign [32, 33].

The goal of the meticulously constructed breast phantom, on the other hand, is to accurately replicate the electromagnetic characteristics and wave propagation characteristics through human breast tissue. This will serve as a vital resource for studies on electromagnetic wave propagation through breast tissue. The phantom's layers, which represent the fat, fibro-glandular tissue, tumor, and breast skin, are all intended to mimic the electromagnetic characteristics of genuine breast tissue, such as permittivity and conductivity. In doing so, a realistic model for modeling and studying the interaction of radiofrequency waves with various tissue types is produced.

## 2 RESEARCH METHODS

### 2.1 Design of proposed antenna

The proposed compact antenna is printed on a Roger 5880 substrate with a standard thickness of 0.8 mm. The antenna has overall dimensions of  $25 \times 25$  mm. Good signal integrity and low signal loss are two of the distinctive electrical qualities of the Rogers 5880 substrate that offer a significant advantage in high-frequency electronics design and implementation, which is one of the main goals of this study. The compact size of the antenna makes it easy to use and has less impact on the infected body, helping in the treatment process of cancer patients. The radiating patch of the antenna consists of a hexagonal shape fed by a 50-ohm feeding line. The proposed antenna used the slotted ground structures to provide larger frequency coverage and perform better in a variety of applications, including communication systems.

The substrate is a vital component in antenna design, and in this instance, Rogers RT5880, a lossy substrate, was selected. Its use is based on its excellent dielectric properties and appropriate loss factors for radio frequency applications. The substrate has a significant impact on the antenna's bandwidth and compactness. The dimensions of the substrate are  $25 \text{ mm} \times 25 \text{ mm}$  on both the X and Y- axes, with a thickness of 0.8 mm. These measurements affect the antenna's overall bandwidth in addition to its resonant frequency and impedance matching. The design of the proposed antenna is shown in Figure 1, where the dimensions of the antenna are shown in Table 1.

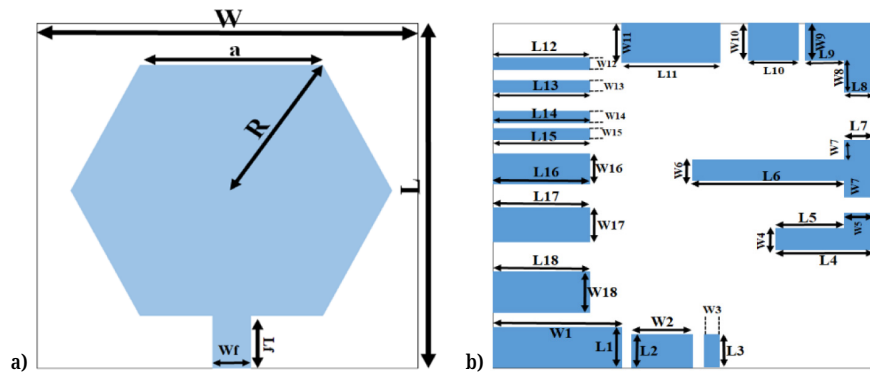


Fig. 1. Proposed antenna (a) top view (b) bottom view

Table 1. Antenna parameters

Parameters	Value (mm)	Parameters	Value (mm)
W	25	L	25
A	11	Wf	2.46
W1	8.5	L1	3
L2	2.5	W3	1.1
W4	1.5	L4	6.5
L5	4.5	W6	1.5
W7	1.5	L7	2
L8	2	W9	2.85
W10	2.85	L10	3.3
L11	6.5	W12	1
W13	0.9	L13	6.5
L14	6.5	W15	0.8
W16	2.2	L16	6.5
L17	6.5	W18	3
R	11	L9	2.5
Lf	2.97	W11	3
W2	4	L12	6.5
L3	2.5	W14	0.8
W5	2	L15	6.5
L6	10	W17	2.7
W8	2.15	L18	6.5

Let us move on to the patch. Made of copper due to its superior electrical conductivity, its six-segmented hexagonal shape is essential in determining the radiation pattern and impedance characteristics of the antenna. The antenna’s resonance frequency and radiating characteristics are determined by the radius, which is set at 12 mm, and its thickness, which is 0.035 mm, which affects surface currents and radiation characteristics. The feed line attaches directly to the patch and has dimensions of 2.46 mm width (X-axis) and 11mm length (Y-axis). It plays a crucial part in insertion loss, impedance matching, and the efficient passage of signals from the feed line to the antenna. Step into the ground plane, which is made of copper annealed and measures 25 × 25 mm

with a 0.035 mm thickness. By adding square and rectangular slots, it hopes to change the way current is distributed, improving bandwidth and the antenna's overall performance. The antenna's emission pattern and impedance are directly impacted by the size of the ground plane. The waveguide's main function is to excite, which helps with signal transfer to the antenna and influences radiation characteristics and efficiency. It guarantees that the antenna is driven effectively at the intended frequencies.

## 2.2 Parametric study of the proposed antenna

When it comes to breast cancer diagnosis, the use of antennas and parametric study represents major advancements in diagnostic techniques. This study explores the intricacies of this parametric analysis, illuminating the crucial function that antennas fulfill in this field. The focal point of this study, the hexagon-shaped patch antenna, shows a dynamic relationship with its radius, represented by the letter R. A crucial component of the study, is closely related to the antennas' current distribution is the choice of R. This decision is crucial since it affects the antenna's performance directly and, in turn, how well breast cancer is detected.

The study methodically examines a variety of R values, each of which adds to a more complex comprehension of the antenna's function. The research's figures visually represent the range of results that correlate to various R values. For researchers and practitioners looking to optimize antenna characteristics for improved breast cancer detection, this thorough analysis provides a road map. Examining the results closely makes the relevance of R especially clear. The report notably emphasizes that an R-value of 11 produces better results than other values. This finding has significant ramifications since it implies that the hexagonal-shaped patch antenna's particular geometric configuration, which is represented by an R of 11, improves its efficacy when it comes to breast cancer detection. The study article explores other pertinent constants in addition to the radius parameter. These could include things such as the gain, polarization properties, and frequency responsiveness of the antenna. The overall effectiveness of the antenna system in capturing and evaluating the properties of breast tissue is influenced by the interaction of these variables. Furthermore, considering the complexity and dynamic character of the human body, the study may investigate the effects of external factors on antenna performance. Variations in physiological circumstances, tissue density, and skin features can all affect how the antenna interacts and, in turn, how accurate breast cancer detection is. The parametric study graph of the proposed antenna is shown in Figure 2.

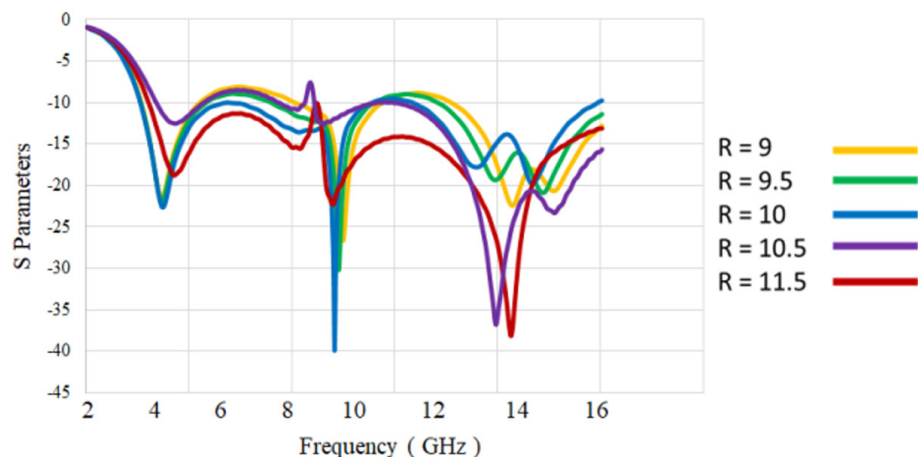


Fig. 2. Parametric studies at different radius of patch

Finally, this parametric study opens new study opportunities into the complex features of antenna performance and design in biomedical applications, in addition to offering insightful information about optimizing a hexagonal-shaped patch antenna for breast cancer detection. The results of this study influence the way that antenna-based technologies are being used in medical diagnostics, encouraging new ideas and improvements in breast cancer detection techniques.

### 2.3 Design of human model

The choice of breast skin as the material is based on its close resemblance to the conductivity and dielectric characteristics of human breast skin. Making this decision is crucial to ensure accurate simulations and studies on the transmission of electromagnetic waves through the breast. The outermost layer of the breast that regulates the first interaction of external electromagnetic waves with the breast is described as a sphere with a center radius of 40 mm and a bottom radius of 40 mm. A permittivity (epsilon) of 38, permeability ( $\mu$ ) of 1, and conductivity of 1.8 (determined at 3 GHz) are some other characteristics.

The fat layer seen on the breast, which has special dielectric properties, is replicated in fat. Given its large thickness and effect on the way waves pass through the breast, fat must be portrayed accurately. The fat layer is represented as a sphere with a 35 mm center radius and a 35 mm bottom radius. This model influences the features of wave propagation through the tissue and provides an accurate representation of the electromagnetic properties of the breast. A permittivity (epsilon) of 5, permeability ( $\mu$ ) of 1, and conductivity of 0.1 (determined at 3 GHz) are further characteristics. The 3D side view of the breast phantom with antenna is shown in Figure 3.

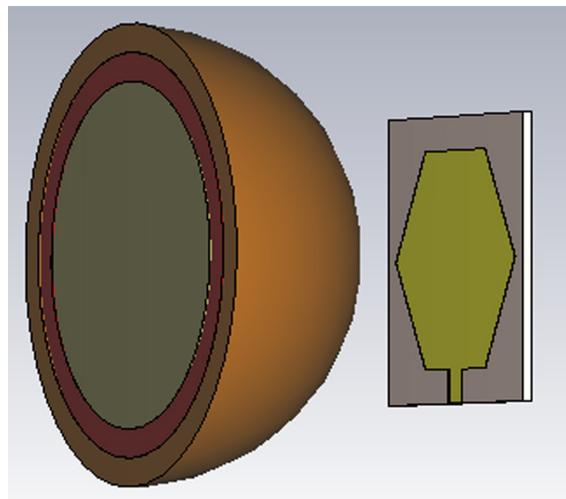


Fig. 3. Side view of the breast phantom with antenna

### 2.4 Design antennas with textile material

To maximize its performance in the medical spectrum, the antenna is constructed utilizing a mix of carefully chosen materials and design specifications. Due to its distinct dielectric properties, the cotton (polyester) substrate affects the antenna's

miniaturization and bandwidth in addition to providing a textile basis appropriate for wearable technology. The form and size of the hexagonal copper patch naturally affect the antenna's radiation pattern and impedance, while also offering minimal losses and dependable signal transmission. Furthermore, the antenna performance is enhanced by the ground plane, which is adorned with square and rectangular slots, by changing the current distribution. Using the CST Studio Suite for modeling, the antenna undergoes a thorough examination over a wide variety of parameters, showing its operational capabilities. The  $S(1,1)$  parameter, which accounts for return loss and the efficiency with which energy is transferred from the transmission line to the antenna, indicates that the optimal working point is at 4.30 GHz and that the effective bandwidth spans 2.423 GHz to 16.0 GHz. Wideband applications require a substantial operational frequency range, which this broad bandwidth exhibits.

### 3 RESULTS AND DISCUSSION

#### 3.1 Results of proposed antenna (S parameters)

The evaluation of a microwave or RF system's ability to reflect power at its input is expressed in terms of the  $S(1,1)$  parameter, which is also known as the input reflection coefficient or return loss. This value is very important for minimizing signal reflection and guaranteeing the best possible power transfer. The complex values that represent  $S(1,1)$ 's magnitude and phase indicate the amplitude and phase shift of the reflected wave, respectively. A system's efficiency is highlighted by a greater negative dB value or a lower  $S(1,1)$  value, which indicates superior system matching and decreased energy reflection. Understanding and reducing reflections become critical factors to improve the efficiency and dependability of RF design applications, such as transmission lines and antennas.

A minimum  $S(1,1)$  value of  $(-38.92)$  dB is revealed by the radiation frequency analysis, showing robust performance qualities. 4.27 GHz is the approved matching frequency. The antenna's effective frequency range is 3.53 GHz to 16.0 GHz, which is the lowest frequency to be found within the frequency range that crosses the  $-10$  dB line. With a maximum of 10% being reflected, this range is known as the effective bandwidth, guaranteeing that at least 90% of the power is transmitted. The  $S$  parameter graph of the proposed antenna is shown in Figure 4.

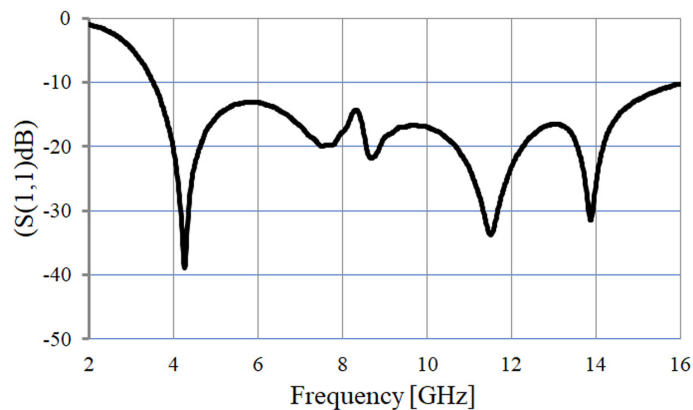


Fig. 4. S parameter of simple antenna

### 3.2 Voltage standing wave ratio

The antenna's minimal voltage standing wave ratio (VSWR) is 1.023, and the frequency that corresponds to that figure is 4.27 GHz. At this frequency, the antenna is operating at its best—that is, absorbing and radiating power as efficiently as possible while reducing reflections back into the system. The antenna is less effective at this frequency, reflecting a significant portion of the incoming power into the system. The VSWR results of the antenna are shown in Figure 5.

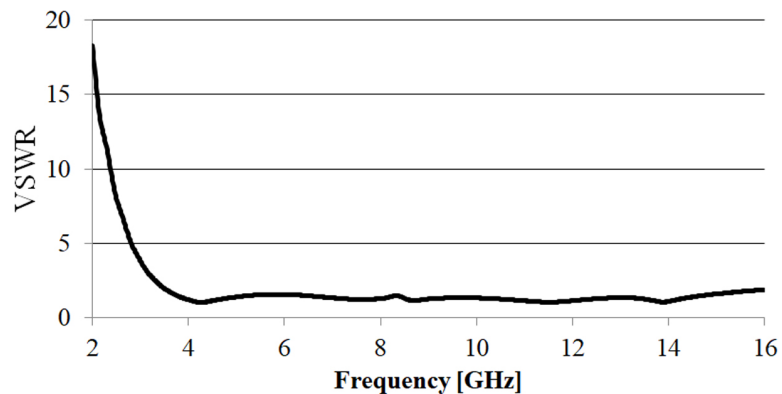


Fig. 5. Voltage standing wave ratio of simple antenna

A VSWR value that is closer to one, particularly in the vicinity of the working frequency, indicates antenna matching. This proximity indicates that the transmission line and the antenna have good impedance matching, which efficiently reduces reflections and maximizes power transfer. A higher VSWR is linked to mismatches and losses, especially close to the working frequency. An imbalance between the transmission line and the antenna, which results in power reflection and ensuing power losses, is indicated by a greater voltage standing wave ratio.

### 3.3 Gain and current distribution

An antenna's gain, expressed in decibels relative to an isotropic radiator (dB), indicates how well it can concentrate radiation in a particular direction. It is an analysis of the antenna of a theoretical isotropic antenna, which radiates in all directions equally. Power is transmitted uniformly in all directions by the isotropic antenna. When assessing antenna performance, gain, which directly affects the coverage area and signal strength, is an important consideration. It is important to keep in mind that a lower gain indicates a wider coverage area with shorter travel times, whereas a greater gain indicates a more directed antenna that can travel farther but has a narrower concentrated region. The spatial variation of electric current along an antenna's conducting parts is referred to as its current distribution. It is essential to comprehend this distribution to analyze radiation patterns and match impedance. An efficient conversion of electrical energy into electromagnetic waves is ensured by proper design, which maximizes the antenna's performance for a given application. The gain and current distribution graph of the antenna is shown in Figures 6 and 7, respectively.



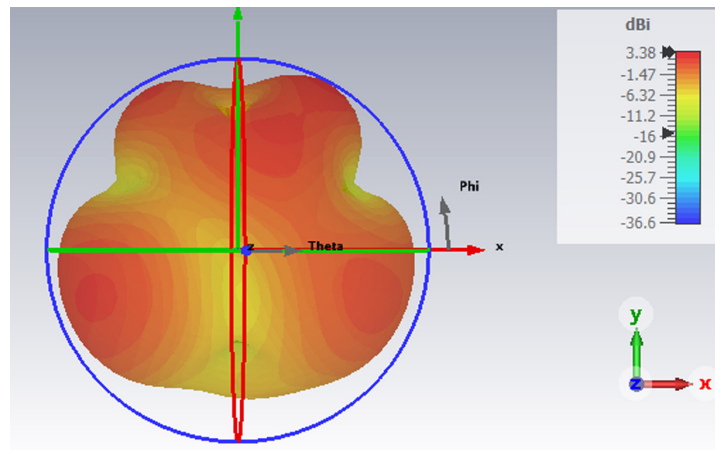


Fig. 6. Gain of the simple antenna

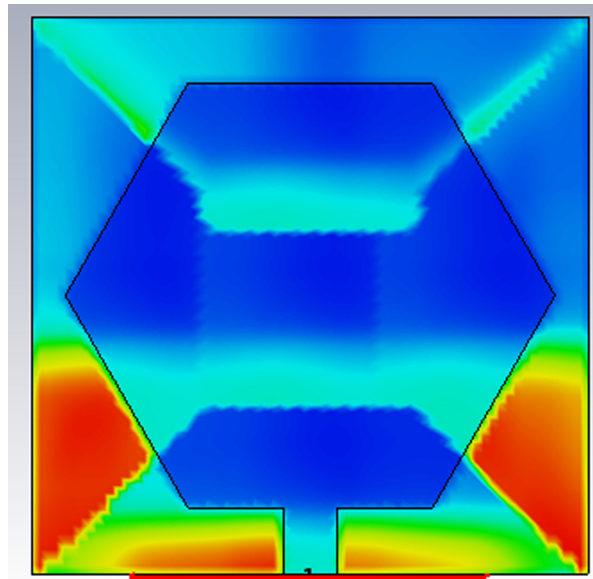


Fig. 7. Current distribution

### 3.4 Results without tumor (S parameter)

The frequency of 3.93 GHz yields the best results for the antenna, and at this frequency, the minimum value of  $S(1,1)$  is measured at  $(-31.37)$  db. The antenna performs exceptionally well at generating and absorbing energy at this frequency while reducing reflection back into the system. Improved impedance matching between the antenna and the transmission line is shown by lower (more negative)  $S(1,1)$  values, which guarantee effective power flow into the antenna with little reflection. 3.38 GHz is the lowest frequency, and 16.0 GHz is the highest frequency in the frequency range that crosses the  $-10$  dB line. Within this range, which is referred to as the antenna's effective bandwidth, a return loss ( $S$  parameter) of less than  $-10$  dB indicates that at least 90% of the power is transmitted and that up to 10% is reflected. Numerous RF applications accept this range as standard. The  $S$  parameters graph of the proposed antenna with healthy tissue is shown in Figure 8.

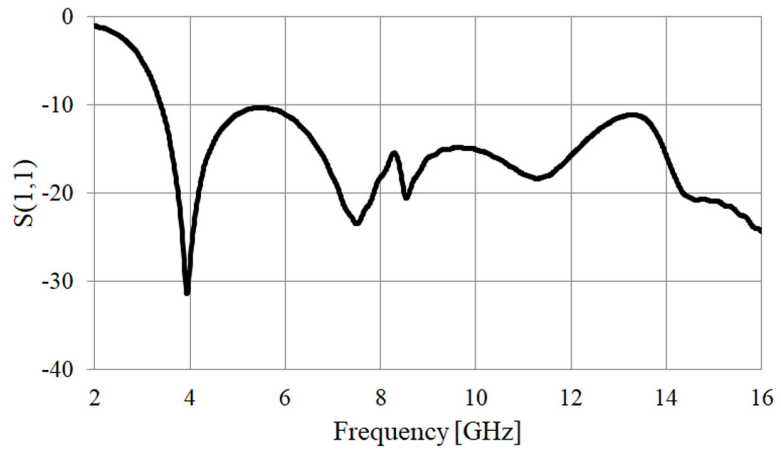


Fig. 8. S parameters with breast healthy tissue

In the case of the highest return loss of (-31.37) dB, 3.93 GHz is still the ideal matching frequency. The optimal frequency for signal transmission is represented as the point of least signal reflection, which is this frequency. Further observations show that the antenna is well-matched to the transmission line in the frequency range of 3.38 GHz to 16.00 GHz when reflections are minimized (below -10 dB).

### 3.5 Results of antennas with textile material

At the matching frequency of 4.30 GHz, the antenna exhibits excellent performance, as evidenced by the measured lowest value of S<sub>11</sub> of (-17.49) dB. By using this frequency, the antenna can produce and absorb energy more effectively while reducing reflection back into the system. At this frequency, lower S<sub>11</sub> values signify better impedance matching between the transmission line and the antenna, which guarantees a higher power transfer into the antenna and lowers reflected energy. The antenna is effective from 2.423 GHz to 16.0 GHz, which is the lowest frequency when looking at the range of frequencies that cross the -10 dB line. This frequency range is referred to as the antenna's effective bandwidth; in several radio frequency applications, a return loss of less than -10 dB indicates at least 90% power transfer and up to 10% reflection.

The ideal matching frequency of 4.30 GHz is in line with the greatest return loss, which is measured at (-17.49) dB. The best signal transmission capabilities of the antenna are indicated by this value, which indicates the place of minimal signal reflection. The S parameters result of the textile-based antenna are shown in Figure 9.

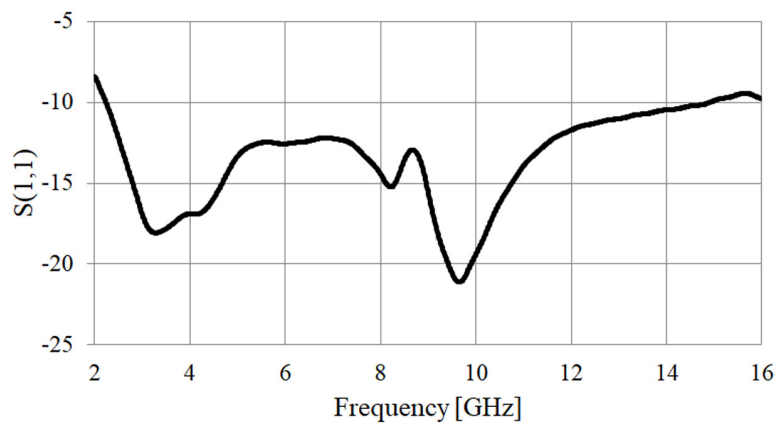


Fig. 9. S parameter of textile based antenna

### 3.6 Results with healthy tissue (textile material)

The following defines the frequency range that includes the lowest and greatest frequencies that cross the  $-10$  dB line: 2.23 GHz is the lowest frequency, while 14.89 GHz is the highest. When the return loss (S parameter) is less than  $-10$  dB, which guarantees at least 90% power transmission and up to 10% reflection, this frequency range is regarded as the antenna's effective bandwidth. This range is commonly used in RF applications. The ideal matching frequency for the highest return loss, measured at  $(-21.13)$  dB, is 9.64 GHz. This frequency indicates the point of least signal reflection and, hence, the point of maximum signal transmission efficiency.

Further data indicates that the antenna can be considered well-matched to the transmission line in the 2.23 GHz to 14.89 GHz frequency range if reflections are reduced to a level below  $-10$  dB. Higher reflections (S (1,1) values nearer 0 dB) raise questions nonetheless regarding the perfection of energy transmission, especially in the lower frequency range. Standing waves could result from this, which could damage the transmitter by creating waves in the transmission line. The antenna's large operating frequency range, which highlights its adaptability, makes it useful for applications that require wideband or multi-band operation, including certain communication and radar systems. This is seen by the wide bandwidth at which S11 is less than  $-10$  dB. The S parameters result of the textile-based antenna with healthy tissue are shown in Figure 10.

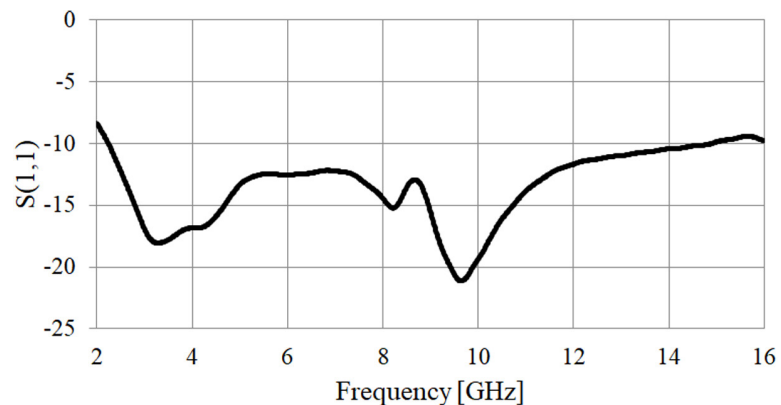
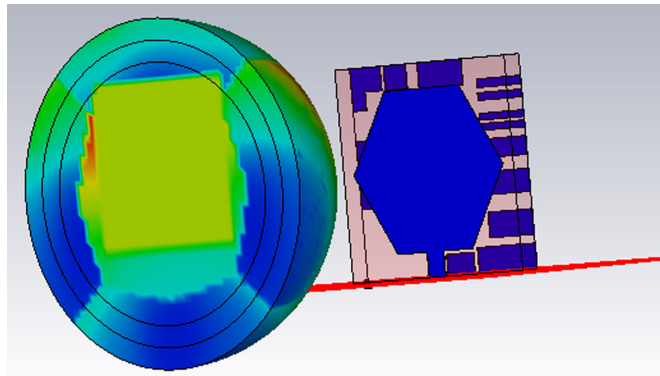


Fig. 10. S parameter with breast healthy tissue

### 3.7 SAR analysis with healthy tissue

In the context of an antenna meant to identify breast tumors, determining the rate at which electromagnetic radiation produced from the antenna is absorbed by the phantom breast tissue is known as a SAR study. SAR, which is measured in watts per kilogram (W/kg), is crucial for ensuring safety and adhering to legal criteria when using electromagnetic fields in medical applications. To detect tumors, the antenna projects electromagnetic waves into the breast phantom; SAR analysis ensures that the energy received by the tissue is within permissible limits to prevent any possible thermal effects. Through the optimization of antenna design to allow excellent tumor identification and safe, low-level electromagnetic tissue exposure, this study contributes to the prioritization of cancer patient safety in diagnostic procedures. SAR analysis of the antenna with healthy is shown in Figure 11.



**Fig. 11.** Back view (specific absorption rate with healthy tissue)

When utilizing an antenna for broadband applications in breast tumor diagnosis, the SAR plays a crucial role in determining how electromagnetic radiation is absorbed by breast tissue. This element conforms to legal criteria and aids in ensuring safety. The data demonstrates a comprehensive SAR examination at 12 GHz with a 0.5 W stimulated power, providing an acceptable power of 0.465915 W, showing a slight variation that could be attributed to reflections or system losses. The volumetric space covered by the analysis is  $-38.8731$  mm to  $38.8731$  mm (x-axis),  $-28.3276$  mm to  $28.3276$  mm (y-axis), and  $-8.32757$  mm to  $60.9776$  mm (z-axis). The volumetric mass and average mass are, respectively,  $1.32908$  times  $10^{-7}$  g and  $0.1$  g.

An absorbed tissue power of  $0.0032319$  W is found inside a tissue volume of  $16741$  mm<sup>3</sup> with a mass of  $0.000251114$  kg and an absorbed power of  $0.0281442$  W. The total SAR, or average rate of energy absorption, is found to be  $12.8702$  W/kg. In a  $0.1$  g tissue mass, the highest SAR is  $21.1439$  W/kg and is found at coordinates  $-8.9375$  mm,  $9.7375$  mm, and  $52.5337$  mm. However, the maximum SAR at the maximum point, which indicates the peak energy absorption rate, is much higher at  $427.726$  W/kg. To protect against any thermal repercussions on the tissue, these numbers—especially the localized maxima—are crucial for understanding and ensuring that the antenna's radiated energy stays below safety limits. Furthermore, antenna settings may be enhanced to better identify tumors and comply with biomedical safety regulations by understanding how SAR is distributed throughout the tissue volume. The computed SAR values demonstrate the electromagnetic waves that the antenna can use to probe breast tissue, and they also show the need to regulate energy absorption to preserve tissue integrity and cancer patient safety when performing diagnostic operations. It took  $122774$  seconds to finish the analysis.

### 3.8 Results with breast-affected tissue (S parameters)

The antenna performs best at  $(-21.13)$  dB, which is the minimal value of  $S(1,1)$  in the radiation frequency domain. The antenna operates most efficiently at  $9.64$  GHz, which is also the frequency at which it generates and absorbs the least amount of reflected energy into the system. The lower (more negative)  $S(1,1)$  values highlight the effectiveness by demonstrating better impedance matching between the transmission line and the antenna. A greater power transfer into the antenna and a decrease in reflected radiation are ensured by this alignment.

When looking at the frequencies that cross the  $-10$  dB line,  $2.25$  GHz is the lowest, and  $14.91$  GHz is the highest. This frequency range is regarded as the antenna's effective bandwidth since it guarantees a return loss ( $S_{11}$  parameter) of less than  $-10$  dB, which translates to at least 90% power transmission and a maximum of 10% reflection.

The ideal matching frequency stays at 9.64 GHz for the maximum return loss, which is measured at  $(-21.13)$  db. At this frequency, the point of maximum signal transmission capacity is indicated by the least amount of signal reflection. Further observations indicate that the antenna is considered well-matched to the transmission line in the 2.25 GHz to 14.91 GHz frequency range when reflections are reduced to a level below  $-10$  db. The S parameters result of the textile-based antenna with affected tissue are shown in Figure 12.

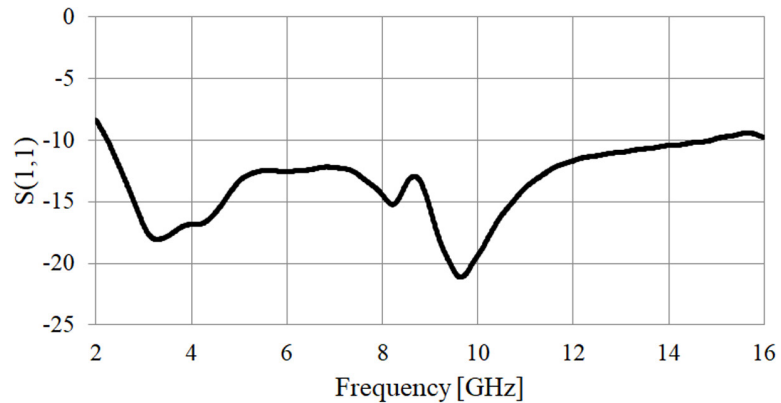


Fig. 12. S parameter with breast-effected tissue

### 3.9 Specific absorption rate analysis with effected tissue

A critical understanding of how biological tissue absorbs electromagnetic radiation required for tumor diagnosis in a phantom breast via the selected antenna is provided by the SAR calculations. In this case, the parameters for the power loss density monitor are 12 GHz, no power scaling, and 0.5 W of stimulated power. The system's reflections and losses could account for the little discrepancy between the stimulated and accepted powers. It is noteworthy that 0.466347 W is the accepted power and the actual power absorbed by the tissue. The measurements of the phantom breast are  $-38.8731$  mm to  $38.8731$  mm on the x-axis,  $-28.3276$  mm to  $28.3276$  mm on the y-axis, and  $-8.32757$  mm to  $60.9776$  mm on the z-axis. The total volume of the phantom breast is  $305270$  ( $\text{mm}^3$ ). With a mass of  $0.000251326$  kg and a volume of  $16755.1$   $\text{mm}^3$ , the tissue inside this volume has an absorbed power of  $0.0280429$  W.  $0.00314924$  W is the power that is either absorbed or stored in the tissue. SAR analysis of the final antenna with affected tissue is shown in Figure 13.

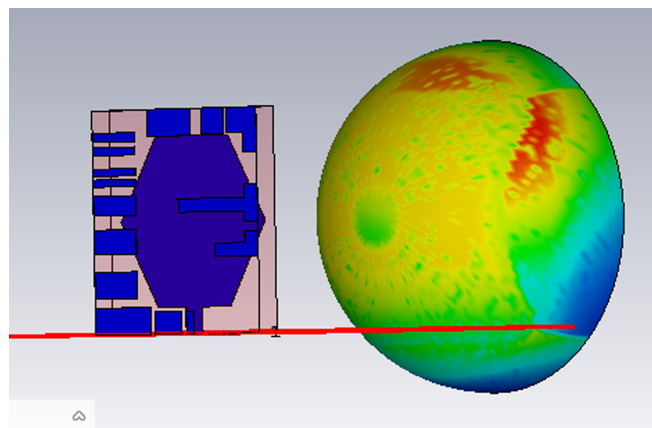


Fig. 13. Antenna front view (specific absorption ratio with effected tissue)

It is critical to assess these SAR values to ensure the security and efficiency of the antenna in medical diagnostics. The location and extent of the maximum SAR within a specific tissue volume provide deeper insights into localized energy absorption, which is crucial for minimizing potential thermal effects and optimizing antenna parameters for safe and successful tumor detection, even though the total SAR and maximum point SAR provide a broad and peak perspective of energy absorption. This SAR study's computation time of 137069 seconds demonstrates a careful and comprehensive computational analysis. This comprehensive SAR analysis made it possible for the developed antenna to meet safety regulations, which is crucial for medical applications where it is necessary to control and limit energy absorption in biological tissues.

The broadband antenna, developed using textile material and meticulously modeled using a phantom breast, represents a significant advancement in the fusion of electromagnetics and biomedical engineering, particularly in the context of non-invasive cancer diagnostics. The antenna demonstrates both technological advancements and a committed effort to enhance the precision and security of cancer identification protocols, with a focus on strict adherence to safety guidelines via an extensive SAR analysis.

#### 4 COMPARISON WITH PREVIOUS RESEARCH

**Table 2.** Performance comparison of proposed antenna with previous research

	Size (mm)	Bandwidth (GHz)	Return Loss	VSWR	Gain
Proposed Antenna	25*25	12.3	-38.92	1.02	3.4
[34]	28*30	5.7	-48	1.003	5.2
[35]	30*25	0.5	-16	1.373	6.45
[36]	80*67	6.6	*	1.05	4.53

Table 2 shows the dimensions of the suggested antenna design, which are 25 mm × 25 mm. Consequently, it exhibits substantial enhancement in terms of compactness and performance metrics compared to previously examined models. As an illustration, the bandwidth of this antenna is 12.3 GHz, which is an enhancement compared to the frequency ranges documented in prior study. In this study [34], the antenna's bandwidth is only 5.7 GHz, which is significantly narrower compared to the achieved bandwidth when implementing the proposed design. The increased bandwidth offered by this novel design enables greater versatility in medical applications, where a wider frequency range is frequently required for accurate signal identification and processing, particularly in the field of medicine. In addition to these factors, another antenna [35] has a bandwidth of only 0.5 GHz, which is significantly less compared to the previous design suggestion. This comparison clearly demonstrates that the new antenna has the capability to properly support a wider variety of frequencies, resulting in improved overall performance.

The suggested antenna has exceptional performance in terms of return loss, which is a crucial characteristic. The measurement is recorded as -38.92 dB, indicating excellent impedance matching and low signal reflection. The return loss of -48 dB stated in [34] is inferior to the proposed design, indicating a lower level of performance. However, it does not guarantee higher performance in all situations. Nevertheless, the suggested antenna's return loss indicates exceptional efficacy

in transmitting signals, which is vital for applications that demand accurate and dependable communication, including medical monitoring and diagnostics.

When assessing the VSWR, the suggested antenna exhibits a remarkably efficient ratio of 1.02, which is the smallest among the models being assessed. In [34], the antenna's VSWR is reported as 1.003, whereas in [36], it is mentioned as 1.05. Additionally, [35] has a VSWR of 1.373. A lower VSWR signifies superior performance and reduced reflected power, which is especially advantageous in medical applications where signal integrity is of utmost importance. Despite having a lower gain of 3.4 dB compared to the gains reported in [35] (6.45 dB) and [34] (5.2 dB), the suggested antenna nevertheless demonstrates competitive performance considering its size and other parameters. The reduced amplification is counterbalanced by the wider range of frequencies and improved reduction of signal reflection, making the suggested antenna a more optimized selection for situations where limitations in size and effectiveness are crucial, such as in small medical equipment. The proposed antenna design exhibits a comprehensive performance that meets the criteria for medical applications, including a small size, broad frequency range, exceptional return loss, and effective voltage standing wave ratio.

## 5 CONCLUSION

The medically engineered antenna is a groundbreaking development in the good health and well-being industry, especially in the areas of tumor detection and therapy. The features of the antenna, including its ability to detect tumors non-invasively and its adherence to strict safety regulations using SAR analysis, represent a major advancement in the field of medical diagnostics. In addition to making the antenna wearable, lightweight, and flexible, the use of textile materials as a substrate also meets the need for continuous monitoring in medical applications. The antenna's versatility and performance are enhanced by its wide bandwidth and hexagonal patch design, and its use of copper assures effective signal transmission with low loss. The thorough design process, which incorporated parametric analysis and testing using a phantom breast model, highlights the dedication to optimizing the antenna's characteristics to satisfy demanding performance requirements. This methodical technique guarantees the antenna's efficacy and dependability in practical medical situations.

Beyond design issues, the antenna's medical applications have a wide range of applications. The antenna shows its worth in improving cancer patient care in various ways, including postoperative surveillance, early tumor diagnosis, and therapy monitoring. Its reach is further increased by its integration with wearable technology and multi-modal diagnostic systems, which enable continuous health monitoring and raise diagnosis accuracy. The antenna's real-world effects on cancer patient outcomes are demonstrated by its practical uses in enhanced mammography systems, postoperative monitoring, and preventive screening programs. The therapeutic uses, such as precision oncology and targeted hyperthermia, highlight the antenna's adaptability and promise to improve medical care. The antenna has several medicinal applications beyond design considerations. It has great promise for enhancing the care of cancer patients in a number of ways, including early tumor detection, post-operative monitoring, and therapeutic monitoring. Continuous health monitoring is made possible by its integration with wearable technology and multi-modal diagnostic systems, which improves diagnosis accuracy. The real-world impact of the antenna on improving cancer patient outcomes is demonstrated by its practical

uses in enhanced mammography systems, postoperative monitoring, and preventive screening programs. Furthermore, the antenna's therapeutic applications—such as targeted hyperthermia and precision oncology—highlight its versatility and promise to transform medical care.

The developed antenna is a technological marvel that also has the potential to revolutionize medical procedures. Its ability to facilitate tailored treatments, advance medical study, and enhance diagnostics makes it an invaluable instrument in the continuous hunt for innovative healthcare solutions.

## 6 REFERENCES




- [1] Q. Li and H. Liu, "Analysis of performance parameters of wearable antenna working near human body," in *2020 IEEE 9th Joint International Information Technology and Artificial Intelligence Conference (ITAIC)*, Chongqing, China, 2020, pp. 1218–1221. <https://doi.org/10.1109/ITAIC49862.2020.9339164>
- [2] C. Fager, T. Eriksson, F. Barradas, K. Hausmair, T. Cunha, and J. C. Pedro, "Linearity and efficiency in 5G transmitters: New techniques for analyzing efficiency, linearity, and linearization in a 5G active antenna transmitter context," *IEEE Microwave Magazine*, vol. 20, no. 5, pp. 35–49, 2019. <https://doi.org/10.1109/MMM.2019.2898020>
- [3] C. Chen, "A uniplanar ultrawideband antenna with unidirectional radiation for WLAN/WiMAX applications," *IEEE Antennas and Wireless Propagation Letters*, vol. 20, no. 5, pp. 743–747, 2021. <https://doi.org/10.1109/LAWP.2021.3061714>
- [4] Z. Zhao, C. Zhang, Z. Lu, and G. Li, "A compact planar UWB antenna with five band-notched characteristics," in *2022 IEEE 10th Asia-Pacific Conference on Antennas and Propagation (APCAP)*, Xiamen, China, 2022, pp. 1–2. <https://doi.org/10.1109/APCAP56600.2022.10068928>
- [5] C. You, J. Choi, H. Ryu, D. Kim, G. Kim, and S. Kim, "Wideband dual-polarized on-board antenna for 5G mm wave mobile application," in *2022 14th Global Symposium on Millimeter-Waves & Terahertz (GSMM)*, Seoul, Republic of Korea, 2022, pp. 195–196. <https://doi.org/10.1109/GSMM53818.2022.9792357>
- [6] H. Chen, Y. Shao, Y. Zhang, C. Zhang, and Z. Zhang, "A low-profile broadband circularly polarized mmwave antenna with special-shaped ring slot," *IEEE Antennas and Wireless Propagation Letters*, vol. 18, no. 7, pp. 1492–1496, 2019. <https://doi.org/10.1109/LAWP.2019.2920875>
- [7] F.-F. Fan, Q.-L. Chen, Y.-X. Xu, X.-F. Zhao, J.-C. Feng, and Z.-H. Yan, "A wideband compact printed dipole antenna array with SICL feeding network for 5G application," *IEEE Antennas and Wireless Propagation Letters*, vol. 22, no. 2, pp. 283–287, 2023. <https://doi.org/10.1109/LAWP.2022.3209326>
- [8] N. Takemura and C. Hata, "An experimental study on half-shaped printed UWB monopole antenna with short stub," in *2021 International Symposium on Antennas and Propagation (ISAP)*, Taipei, Taiwan, 2021, pp. 1–2. <https://doi.org/10.23919/ISAP47258.2021.9614549>
- [9] B. Mohamadzade, R. B. V. B. Simorangkir, R. M. Hashmi, Y. Chao-Oger, M. Zhadobov, and R. Sauleau, "A conformal band-notched ultrawideband antenna with monopole-like radiation characteristics," *IEEE Antennas and Wireless Propagation Letters*, vol. 19, no. 1, pp. 203–207, 2020. <https://doi.org/10.1109/LAWP.2019.2958036>
- [10] C. You, Y. He, W. Li, L. Zhang, S.-W. Wong, and Z. Zhou, "Design of slot-coupled broadband 5G mm wave base station antenna based on double-layer patch," in *2022 IEEE MTT-S International Microwave Workshop Series on Advanced Materials and Processes for RF and THz Applications (IMWS-AMP)*, Guangzhou, China, 2022, pp. 1–3. <https://doi.org/10.1109/IMWS-AMP54652.2022.10106844>






- [11] H. Hu *et al.*, “Compact planar inverted-f antenna for microsats omnidirectional communications,” *IEEE Antennas and Wireless Propagation Letters*, vol. 20, no. 2, pp. 160–164, 2021. <https://doi.org/10.1109/LAWP.2020.3042215>
- [12] B. R. Sanju Priya and G. Anitha, “Simulation and comparison of RF performance of the novel inverted F SIW antenna with triangular split rings SIW antenna for X band applications,” in *2023 Eighth International Conference on Science Technology Engineering and Mathematics (ICONSTEM)*, Chennai, India, 2023, pp. 1–6. <https://doi.org/10.1109/ICONSTEM56934.2023.10142658>
- [13] S. Sarjoghian, Y. Alfadhil, and X. Chen, “Compact ultra-wideband double-ridged horn antennas for medical imaging,” in *2016 Loughborough Antennas & Propagation Conference (LAPC)*, Loughborough, UK, 2016, pp. 1–4. <https://doi.org/10.1109/LAPC.2016.7807516>
- [14] J. Sachs, M. Helbig, S. Ley, P. Rauschenbach, M. Kmec, and K. Shilling, “Short interfacial antennas for medical microwave imaging,” in *2017 International Workshop Antenna Technology: Small Antennas, Innovative Structures, and Applications (IWAT)*, 2017, pp. 1–4. <https://doi.org/10.1109/IWAT.2017.7915370>
- [15] M. Darabi and F. Mohajeri, “An efficient and compact monopole antenna backed with square loop EBG structure for medical wireless body area network applications,” *Radio Science*, vol. 57, no. 1, pp. 1–19, 2022. <https://doi.org/10.1029/2021RS007335>
- [16] A. Abatal, M. Mzili, T. Mzili, K. Cherrat, A. Yassine, and L. Abualigah, “Intelligent interconnected healthcare system: Integrating IoT and big data for personalized patient care,” *International Journal of Online and Biomedical Engineering (iJOE)*, vol. 20, no. 11, pp. 46–65, 2024. <https://doi.org/10.3991/ijoe.v20i11.49893>
- [17] K. N. Olan-Nuñez, R. S. Murphy-Arteaga, and M. Alibakhshikenari, “Dual-band Slot-SSR antenna on PLA-printed substrate for 2.4/5.8 GHz ISM-Band Internet of Things (IoT) applications,” in *2022 IEEE 8th World Forum on Internet of Things (WF-IoT)*, Yokohama, Japan, 2022, pp. 1–6. <https://doi.org/10.1109/WF-IoT54382.2022.10152048>
- [18] A. I. O. Abdullah, A. M. Algatlawi, and B. Alameen, “Decoupling of compact MIMO antennas using parasitic element and electromagnetic band gap structure,” in *2023 IEEE 3rd International Maghreb Meeting of the Conference on Sciences and Techniques of Automatic Control and Computer Engineering (MI-STA)*, Benghazi, Libya, 2023, pp. 702–706. <https://doi.org/10.1109/MI-STA57575.2023.10169823>
- [19] M. M. Taqdeer, Q. M. Amjad, M. Zahid, and Y. Amin, “2\*2 Hexagonal-shaped antenna array for 5.8 GHz ISM band applications,” in *2023 7th International Multi-Topic ICT Conference (IMTIC)*, Jamshoro, Pakistan, 2023, pp. 1–4. <https://doi.org/10.1109/IMTIC58887.2023.10178485>
- [20] V. Asha and K. Bhavanishankar, “Towards efficient lung cancer detection: V-Net-based segmentation of pulmonary nodules,” *International Journal of Online and Biomedical Engineering (iJOE)*, vol. 20, no. 11, pp. 31–45, 2024. <https://doi.org/10.3991/ijoe.v20i11.49165>
- [21] H. González, C. J. Arizmendi, and B. F. Giraldo, “Development of a deep learning model for the prediction of ventilator weaning,” *International Journal of Online and Biomedical Engineering (iJOE)*, vol. 20, no. 11, pp. 161–178, 2024. <https://doi.org/10.3991/ijoe.v20i11.49453>
- [22] M. Cabanillas-Carbonell and J. Zapata-Paulini, “Improving the accuracy of oncology diagnosis: A machine learning-based approach to cancer prediction,” *International Journal of Online and Biomedical Engineering (iJOE)*, vol. 20, no. 11, pp. 102–122, 2024. <https://doi.org/10.3991/ijoe.v20i11.49139>
- [23] Y. I. A. Al-Yasir *et al.*, “A new and compact wide-band microstrip filter-antenna design for 2.4 GHz ISM band and 4G applications,” *Electronics*, vol. 9, no. 7, p. 1984, 2020. <https://doi.org/10.3390/electronics9071084>




- [24] M. Zahid, M. M. Taqdeer, and Y. A. Amin, "Compact dual-band microstrip patch antenna for C- and X- and Ku-band applications," *Eng. Proc.*, vol. 46, no. 1, p. 16, 2023. <https://doi.org/10.3390/engproc2023046016>
- [25] P. Anagnostopoulou and A. Drigas, "Social robots, mindfulness, and kindergarten," *International Journal of Online and Biomedical Engineering (iJOE)*, vol. 20, no. 11, pp. 146–160, 2024. <https://doi.org/10.3991/ijoe.v20i11.49503>
- [26] J.-F. Qian, F.-C. Chen, K.-R. Xiang, and Q.-X. Chu, "Resonator-loaded multi-band microstrip slot antennas with bidirectional radiation patterns," *IEEE Trans. Antennas Propag.*, vol. 67, no. 10, pp. 6661–6666, 2019. <https://doi.org/10.1109/TAP.2019.2927621>
- [27] "5.8 GHz the best choice for RTLS," purelink, [online]. Available: <http://www.purelink.ca/en/technologies/real-time-location-system.php> [Accessed: April 2019]
- [28] K. Li, L.-J. Xu, Z. Duan, Y. Tang, and Y. Bo, "Dual-band and dual-polarized repeater antenna for wearable applications," in *2018 IEEE MTT-S International Wireless Symposium (IWS)*, 2018, pp. 1–3. <https://doi.org/10.1109/IEEE-IWS.2018.8400852>
- [29] Y.-L. Li and K.-M. Luk, "Low-cost 3-D printed THz open resonator antenna," *IEEE Antennas Wirel. Propag. Lett.*, vol. 22, no. 1, pp. 84–88, 2023. <https://doi.org/10.1109/LAWP.2022.3202927>
- [30] J. Zhu, Y. Yang, Z. Hou, S. Liao, and Q. Xue, "Aperture-shared all-metal end-fire high gain parabolic antenna for millimeter-wave multi-beam and Sub-6 GHz communication applications," *IEEE Trans. Antennas Propag.*, vol. 71, no. 3, pp. 2784–2789, 2023. <https://doi.org/10.1109/TAP.2022.3232439>
- [31] J. Wang and J. Xu, "Environmental implications of PCB manufacturing in China," in *Proceedings of the IEEE International Symposium on Electronics and the Environment*, 2004, pp. 156–158.
- [32] D. Helena, A. Ramos, T. Varum, and J. Matos, "Antenna design using modern additive manufacturing technology: A review," *IEEE Access*, vol. 8, pp. 177064–177083, 2020. <https://doi.org/10.1109/ACCESS.2020.3027383>
- [33] M. Khosravani and T. Reinicke, "On the environmental impacts of 3D printing technology," *Appl. Mater. Today*, vol. 20, p. 100689, 2020. <https://doi.org/10.1016/j.apmt.2020.100689>
- [34] S. Bhavani and T. Shanmuganatham, "Wideband fabric antenna for ultra-wideband applications using for medical applications," *Defence Science Journal*, vol. 72, no. 6, pp. 864–872, 2022. <https://doi.org/10.14429/dsj.72.17919>
- [35] A. Y. I. Ashyap *et al.*, "Robust and efficient integrated antenna with EBG-DGS enabled wide bandwidth for wearable medical device applications," *IEEE Access*, vol. 8, pp. 56346–56358, 2020. <https://doi.org/10.1109/ACCESS.2020.2981867>
- [36] R. B. V. B. Simorangkir, A. Kiourti, and K. P. Esselle, "UWB wearable antenna with a full ground plane based on PDMS-embedded conductive fabric," *IEEE Antennas and Wireless Propagation Letters*, vol. 17, no. 3, pp. 493–496, 2018. <https://doi.org/10.1109/LAWP.2018.2797251>

## 7 AUTHORS

**Amer Alsaraira**    holds a PhD in Biomedical Engineering from Monash University since the year 2009. He is currently an assistant professor at the Biomedical Engineering Department at German Jordanian University-Jordan since 9/2022. He teaches various courses for the undergraduate students, supervises their graduation projects, and is a member of many committees at the department. His

current research is in the fields of modeling and simulation of biomedical systems, wireless networks, and DSP (E-mail: [amer.alsaraira@gju.edu.jo](mailto:amer.alsaraira@gju.edu.jo)).

**Omar A. Saraereh**    received Ph.D. degree in Electrical and Electronic Engineering from Loughborough University, U.K., in 2005. He is currently a full professor with the Department of Electrical Engineering, Hashemite University, Jordan. He has published many articles in various international journals and conferences (E-mail: [eloas2@hu.edu.jo](mailto:eloas2@hu.edu.jo)).

**Samer Alabed**    is currently an associate professor, the director of the accreditation and quality assurance center, and the director of the e-learning and academic performance improvement center at the German Jordanian University, Jordan. Further information is available on his homepage: <http://drsamer.alabed.wixsite.com/samer> (E-mail: [samer.alabed@gju.edu.jo](mailto:samer.alabed@gju.edu.jo)).